Urinary 8-OHdG and MDA as rapid biodosimetry markers in the lethal/sublethal dose range

SATORU MONZEN[1,2], KENJI TERADA[1], YUSUKE TAWATA[1], TAKANORI SATO[1], NOZOMI KOUSAKA[1] and YASUSHI MARIYA[3]

[1]Department of Radiation Science, Hirosaki University Graduate School of Health Sciences, Hirosaki, Aomori 036-8564, Japan; [2]Research Center for Biomedical Sciences, Hirosaki University, Hirosaki, Aomori 036-8564, Japan; [3]Center for Cancer Treatment and Examination, Aomori Rosai Hospital, Hachinohe, Aomori 031-8551, Japan

Received September 30, 2025; Accepted March 13, 2026

DOI: 10.3892/mmr.2026.13884

Abstract. Rapid and accurate assessment of ionizing radiation exposure is essential for effective triage in acute radiation syndrome. However, although several biodosimetry approaches are available (such as clinical signs, routine laboratory markers and cytogenetic assays), rapid and scalable dose stratification remains challenging in large-scale emergencies. The present study evaluated two oxidative stress-related urinary metabolites, 8-hydroxy-2'-deoxyguanosine (8-OHdG) and malondialdehyde (MDA), as candidate biomarkers in the high-dose exposure range. Male C57BL/6NJcl mice (8 weeks) received whole-body X-irradiation (0-10 Gy at 1.0 Gy/min). Urine samples were collected at 24 or 72 h postexposure. Urinary 8-OHdG was quantified using a lateral flow immunochromatographic assay (with ELISA validation) and MDA levels were measured using a thiobarbituric acid-reactive substances assay. Values were normalized to creatinine. Tissue distribution was assessed across multiple organs, and bone marrow cell cultures were used to examine extracellular release and to support tissue-origin inference under controlled conditions. Bone marrow injury was evaluated by flow cytometry detection of apoptotic cells. Urinary 8-OHdG and MDA levels increased dose-dependently, with significant correlations (8-OHdG: r=0.55 at 24 h, r=0.50 at 72 h; MDA: r=0.65 at 24 h, r=0.50 at 72 h; all $P<0.05$). A sharp rise occurred at ≥7 Gy, where 8-OHdG levels rose 3.7-fold and MDA levels rose 2.3-fold relative to controls. Tissue analyses identified the bone marrow and spleen as primary sources. *In vitro* bone marrow cultures confirmed dose-dependent release, while cell death profiling indicated a shift toward necrosis at high doses. Together, these findings supported the potential utility of urinary 8-OHdG and MDA as rapid and noninvasive biomarkers for early risk stratification in radiation emergencies.

Correspondence to: Professor Satoru Monzen, Department of Radiation Science, Hirosaki University Graduate School of Health Sciences, 66-1 Hon-cho, Hirosaki, Aomori 036-8564, Japan
E-mail: monzens@hirosaki-u.ac.jp

Key words: ionizing radiation, acute radiation syndrome, biodosimetry, urinary biomarkers, 8-hydroxy-2'-deoxyguanosine, malondialdehyde

Introduction

Accidental or unintended exposure to high doses of ionizing radiation (IR) can result in acute radiation syndrome (ARS), marked by depletion of radiosensitive progenitor cells in the bone marrow, gastrointestinal tract, and skin (1). The severity of ARS and clinical outcome depend on timely dose assessment and therapeutic intervention, particularly in the moderate-to-high dose range. International guidance documents from the WHO, IAEA, and NATO, together with coordinated networks such as RENEB, describe the use of clinical assessment, laboratory parameters, and cytogenetic/molecular approaches for radiation triage (2-5). However, several higher-precision biodosimetric approaches require specialized infrastructure and/or processing time, which can limit rapid and scalable dose stratification in large-scale exposure scenarios. For example, chromosomal aberration assays, a widely used reference method for biological dosimetry, typically require lymphocyte culture and metaphase preparation over several days and are therefore not optimal for immediate triage (3,6). These limitations highlight the urgent need for noninvasive, rapid, and reliable biodosimetry methods. Urine represents an attractive biofluid for this purpose: collection is simple and noninvasive, and urinary metabolites reflect systemic biochemical alterations (7). Radiation metabolomics studies in rodents and nonhuman primates have shown IR-induced perturbations of urinary profiles, supporting the concept of urinary metabolites as biomarkers for dose assessment (8,9).

Oxidative stress is a key mediator of IR-induced injury. Ionization of water by IR generates hydroxyl radicals and other reactive oxygen species (ROS) that damage cellular macromolecules. Guanine, the DNA base most susceptible to oxidation, is converted to 8-hydroxy-2'-deoxyguanosine (8-OHdG), which is excised during base excision repair and subsequently excreted in urine (10,11). Peroxidation of

polyunsaturated fatty acids similarly yields malondialdehyde (MDA), a stable aldehyde end product widely used as an indicator of lipid peroxidation (12,13). Both 8-OHdG and MDA have been employed as oxidative stress biomarkers in diverse conditions, including smoking, cardiovascular disease, and ischemia (14,15). Recent studies have highlighted the reproducibility of urinary 8-OHdG (16) and its potential utility as a marker of medical radiation exposure (17,18). In contrast, evidence is limited for lethal or near-lethal whole-body exposure scenarios, particularly in animal ARS models. Most prior investigations of urinary 8-OHdG have focused on human low-dose diagnostic procedures, radiotherapy, or occupational exposure, typically below 5 Gy (17,19). Data on urinary MDA following IR are also scarce, with most reports restricted to UV exposure or chemical models of oxidative stress (20). Therefore, whether these metabolites show dose-responsive, threshold-like increases after high-dose whole-body irradiation in a murine ARS model has yet to be demonstrated.

Building on this rationale, we hypothesized that urinary 8-OHdG and MDA could serve as rapid biomarkers of high-dose IR exposure. We therefore examined their dose- and time-dependent changes in mice subjected to whole-body X-irradiation, traced their tissue origins, and evaluated bone marrow injury as a mechanistic correlate. The aim of this study was to determine whether these oxidative-stress metabolites can be developed as noninvasive biodosimetry tools suitable for triage in radiation emergencies.

Materials and methods

Animals and irradiation. Male C57BL/6NJcl mice (CLEA Japan Inc., Tokyo, Japan) were obtained at 7 weeks of age, acclimatized for one week, and used at 8 weeks. Total-body irradiation was performed using an MBR-1520R-3 X-ray generator (Hitachi Medical Corp., Tokyo, Japan) operating at 150 kVp, 20 mA, and 1.0 Gy/min, equipped with 0.5-mm Al and 0.3-mm Cu filters. The source-to-animal or -cell culture medium distance was fixed at 45 cm, and mice were irradiated in a ventilated acrylic holder with standardized positioning to minimize dose inhomogeneity. Dose rate and output were verified before each irradiation session using a calibrated ionization chamber dosimeter (model TN31013; PTW, Freiburg, Germany) with calibration traceable to national standards (calibration performed annually). Mice received 0, 2, 4, 6, 7, and 10 Gy and were deeply anesthetized with isoflurane (induction, 4-5%; maintenance, 2-3%) at 24 or 72 h after exposure and subsequently euthanized by cervical dislocation. Each dose group consisted of n=5-8 mice per time point. The exact n for each dose/time point is provided in the corresponding figure legends.

Animal husbandry and sampling conditions. Mice were housed under standard specific-pathogen-free conditions with a controlled temperature and humidity and a 12-h light/dark cycle. Animals had ad libitum access to standard chow and water. Urine was collected immediately before euthanasia at the scheduled time points (24 or 72 h post-irradiation) during routine handling, without fasting and without abdominal compression.

Urine and tissue collection. Urine was collected immediately before euthanasia from spontaneously voided samples during routine handling, without abdominal compression. Blood and tissues/organs (liver, kidney, lung, intestine, spleen, muscle, and femoral bone marrow) were harvested, and homogenized using BioMasher II (cat. no. 893062; Nippi Inc., Tokyo, Japan) in an appropriate volume of lysis buffer (cat. no. 295-73901; LysoPure™ Nuclear and Cytoplasmic Extractor Kit, FUJIFILM Wako Pure Chemical Corp., Miyazaki, Japan), and stored at -80˚C until analysis. Using the LysoPure™ Nuclear and Cytoplasmic Extractor Kit, nuclear and cytoplasmic fractions were separated according to the manufacturer's protocol. Nuclear fractions were used for DNA extraction and subsequent 8-OHdG analysis, whereas cytoplasmic fractions containing proteins were used for TBARS quantification. Extracted DNA was enzymatically hydrolyzed using nuclease P1 (FUJIFILM Wako Pure Chemical Corp.) and alkaline phosphatase (Sigma-Aldrich, St. Louis, MO, USA) according to the manufacturers' instructions prior to ELISA quantification. For tissue distribution analysis, organs were collected from the control (0 Gy) and 7 Gy groups at 24 h after irradiation. The experimental workflow is illustrated in Fig. 1.

Rationale for time points and in vitro doses. The 24 and 72-h sampling time points were selected to capture biologically distinct post-exposure windows relevant to ARS. In humans, the prodromal phase typically occurs within hours to the first 1-2 days after exposure, followed by a latent phase and subsequent manifest illness depending on dose (21-23). In murine models, hematopoietic injury evolves comparatively rapidly, and early biological alterations are detectable within the first several days after total-body irradiation (19). Therefore, 24 h was chosen to reflect an early phase dominated by acute oxidative injury, whereas 72 h was chosen to reflect a later phase when systemic responses and evolving hematopoietic injury contribute to biomarker dynamics. The 48-h interval was not included because it represents an intermediate stage between these two phases and was not expected to provide substantially different mechanistic information beyond 24 and 72 h within the scope of this study. For the *in vitro* bone marrow experiments, doses were selected to span moderate-to-high injury conditions while maintaining assay interpretability: 0-4 Gy was used to evaluate dose-responsive extracellular release under viable culture conditions, and 7 Gy was included to align with the *in vivo* threshold-like response (≥7 Gy) and to explore changes under severe injury where necrosis becomes more prominent. In C57BL/6 mice, whole-body irradiation in the range of approximately 7-9 Gy has been reported to induce severe hematopoietic injury and high mortality within 30 days, depending on dose rate and supportive care conditions (24,25).

Creatinine normalization. Urinary creatinine concentrations were measured using a lateral flow immunochromatographic assay (Techno Medica Co., Yokohama, Japan) to enable correction for urine dilution. Urinary 8-OHdG and MDA levels were normalized to creatinine and expressed as ng/mg creatinine or μM/mM creatinine.

Quantification of urinary 8-OHdG. Urinary 8-OHdG was quantified using a lateral flow immunochromatographic assay

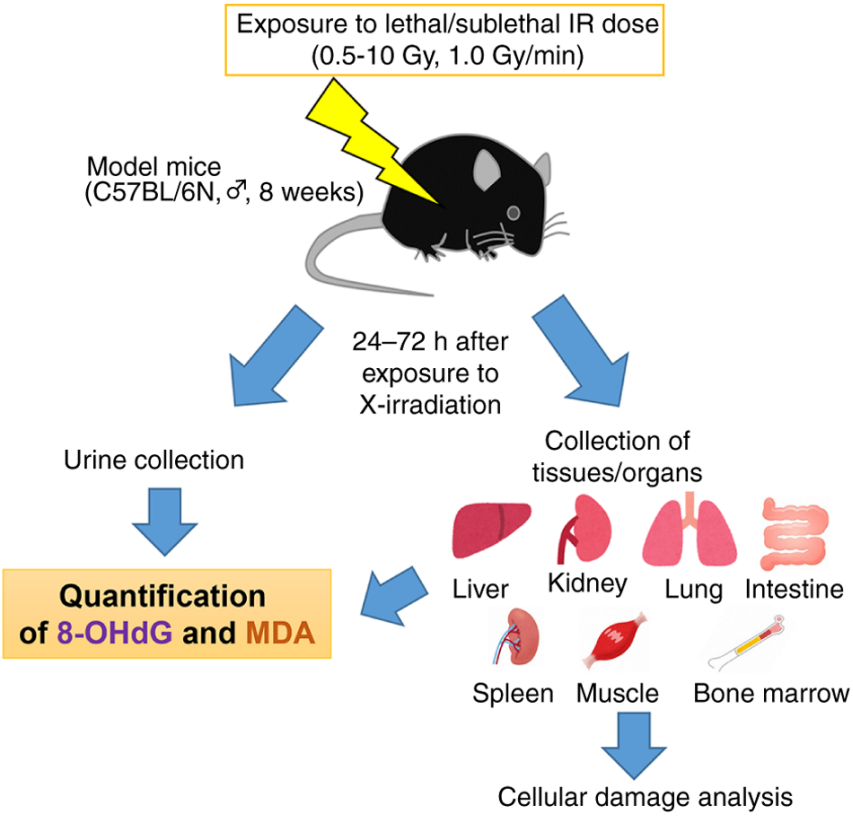

Figure 1. Experimental workflow of the mouse model exposed to lethal and sublethal doses of ionizing radiation (0-10 Gy at 1.0 Gy/min). Urine and organs (liver, kidney, lung, intestine, spleen, muscle and bone marrow) were collected at 24-72 h postexposure. Urinary 8-OHdG and MDA levels were quantified, and cellular damage analyses were performed. 8-OHdG, 8-hydroxy-2'-deoxyguanosine; IR, ionizing radiation; MDA, malondialdehyde.

and verified by ELISA (cat. no. KOG-200SE; NIKKEN SEIL Co., Shizuoka, Japan). Absorbance was read at 450 nm. Unless otherwise stated, all quantitative values reported in this study are based on the immunochromatographic assay, and ELISA was used for methodological verification in a subset of samples.

Quantification of urinary MDA. Urinary MDA levels were determined using a TBARS assay kit (cat. no. NWK-MDA01; Northwest Life Science Specialties, Vancouver, WA, USA), with optical density recorded at 530 nm. To minimize non-specific background in the TBARS assay, all samples and standards were processed in parallel with reagent blanks and kit-provided standards according to the manufacturer's protocol. Absorbance was measured within the recommended time window, and results were calculated using the standard curve. Each assay run included internal quality controls, and samples were analyzed in duplicate; when replicate values differed beyond an acceptable range, the measurement was repeated. Because TBARS detects multiple thiobarbituric acid-reactive species, the values are interpreted as TBARS (MDA equivalents) rather than absolute MDA.

Quantification of tissue 8-OHdG and MDA. Because immunochromatographic assays are optimized for urine matrices, 8-OHdG levels in tissue homogenates and cell culture supernatants were quantified using a commercially available ELISA kit (NIKKEN SEIL Co.) according to the manufacturer's instructions. Tissue 8-OHdG levels were expressed as μmol/mg DNA. For MDA analysis, freshly prepared tissue homogenates were subjected to the TBARS assay (Northwest Life Science Specialties), and results were normalized to total protein concentration and expressed as μmol/mg protein.

Bone marrow cell culture and extracellular marker analysis. Bone marrow cells were flushed from both femurs of mice (n=4 mice per experiment) and processed individually, cultured in RPMI-1640 medium supplemented with 10% fetal bovine serum and 1% penicillin-streptomycin, and irradiated under the same conditions as *in vivo* at 0, 2, 4, and 7 Gy. Culture supernatants were collected 24 h after exposure for 8-OHdG and MDA analysis. For normalization of culture supernatant measurements, results were expressed per $5x10^6$ cells at the time of supernatant collection. Cell numbers were determined at the time of supernatant collection using a hemocytometer (Bürker-Türk hemocytometer, Erma, Inc., Saitama, Japan) with trypan blue exclusion. In addition to extracellular 8-OHdG/MDA quantification, bone marrow cell death profiles (Annexin V/PI) and DNA damage (comet assay) were evaluated as described below.

Apoptosis and necrosis assays. Bone marrow cells were stained with Annexin V-FITC (cat. no. 640905; BioLegend, San Diego, CA, USA) and propidium iodide (PI) (cat. no. 421301; BioLegend) and analyzed by flow cytometry (FACS Aria SORP, BD Biosciences, San Jose, CA, USA). Cell populations were classified as viable (Annexin V^-/PI^-), early apoptotic

(Annexin V^+/PI^-), late apoptotic (Annexin V^+/PI^+), or necrotic (Annexin V^-/PI^+). Debris was excluded based on forward and side scatter characteristics, and doublets were removed using FSC-A/FSC-H gating prior to apoptosis/necrosis analysis.

Detection of DNA fragments. The Comet Assay Single Cell Gel Electrophoresis Assay (cat. no. 4250-050-K; R&D Systems, Inc., Minneapolis, MN, USA) was used to evaluate the DNA fragments of the cells irradiated with IR. One day after seeding in a culture dish at a concentration of $1.0x10^5$ cells/ml, the cells were irradiated with 0.1 and 7 Gy of X-rays, and the cells were collected after 24 h. These two doses were selected to represent a low-dose reference and a severe-injury condition corresponding to the *in vivo* threshold response (≥7 Gy), while limiting assay burden. The 24-h time point was chosen to capture early DNA damage during the acute phase, consistent with the primary urine biomarker assessment. The 0.1 Gy dose was included as a low-dose control to evaluate sublethal DNA damage, whereas 7 Gy represented a high-dose condition associated with severe hematopoietic injury. The collected cells were fixed on glass slide (Matsunami Grass Inc., Osaka, Japan) using LM Agarose (R&D Systems, Inc.). The glass slide to which the sample was attached was immersed in an alkaline solution [200-mM NaOH, 1-mM ethylenediaminetetraacetic acid (EDTA)], and electrophoresis (21 V, 3 A, 30 min, 4˚C) was performed. After washing the glass slide with distilled water and 70% EtOH and drying, it was stained with 100 μl of a staining solution containing a mixture of SYBR Green (R&D Systems, Inc.) and TE Buffer (10-mM Tris, 1-mM EDTA). After drying, the tail moment was observed using a fluorescence microscope (iX71; OLYMPUS Inc., Tokyo, Japan). Images were taken using Comet Assay IV (Instem, Conshohocken, USA) for observation purposes. Tail moment was calculated using the formula: Tail moment=Tail length x (% tail DNA)/100, using Comet Assay IV software. This calculation reflects both the extent and the intensity of DNA fragmentation in individual cells. For each animal, at least 50-100 cells were analyzed, and a total of 250-800 cells per dose group were included in the analysis.

Normalization and units. Urinary biomarkers were normalized to creatinine to account for variation in urine concentration. Tissue biomarkers were normalized to DNA or protein content to correct for differences in tissue mass and extraction yield. These normalization strategies were selected according to the biological matrix analyzed. Supernatant measurements from *in vitro* bone marrow cultures were normalized to cell number and expressed per $5x10^6$ cells, to reflect extracellular release per unit cell number. Because these matrices represent biologically distinct compartments, unit standardization across sample types was not appropriate; instead, normalization was performed according to established conventions for each specimen type.

Statistical analysis. Data are presented as mean ± standard deviation unless otherwise stated. Group differences were assessed using an unpaired t-test or one-way ANOVA followed by the Tukey-Kramer test for multiple comparisons, as appropriate. Formal normality testing was not performed because of the relatively small sample sizes in several groups (n=5-8), for which normality tests have limited statistical power and may be difficult to interpret reliably. Associations between radiation dose (treated as a continuous variable for dose-response analysis, although administered at discrete levels) and biomarker concentrations were examined using Pearson's correlation coefficient; to reduce dependence on distributional assumptions, Spearman's rank correlation was additionally performed as a non-parametric sensitivity analysis. For dose-response visualization, linear and quadratic regression models were tested. Model selection was based on goodness-of-fit (R^2) and residual patterns, while prioritizing parsimony to avoid overfitting; therefore, the linear model was used unless the quadratic model provided a higher R^2 with an improved residual pattern. Receiver operating characteristic (ROC) curve analysis was performed to evaluate the ability of biomarkers to discriminate between dose categories, and the area under the curve (AUC) was calculated. Statistical significance was set at $P<0.05$. All analyses were conducted using OriginPro 2016 (OriginLab, Northampton, MA, USA) and the Statcel 3 add-in for Microsoft Excel (OMS Publishing Inc., Saitama, Japan).

Results

Dose- and time-dependent increase in urinary 8-OHdG and MDA levels. Urinary biomarkers are reported as creatinine-normalized concentrations to account for urine dilution, whereas tissue and culture supernatant measurements are normalized to DNA/protein content or cell number, respectively, reflecting matrix-appropriate normalization (see Materials and Methods). Urinary 8-OHdG remained stable up to 4 Gy but increased sharply at higher doses, showing a threshold-like rise at ≥7 Gy (Fig. 2A and B). Post hoc comparisons indicated that the first statistically significant increase occurred at ≥7 Gy at both 24 and 72 h. At 7 Gy, urinary 8-OHdG increased 6.25-fold at 24 h and 2.10-fold at 72 h relative to controls ($P=3.62x10^{-4}$ and $P=2.54x10^{-2}$, respectively), and a comparable increase was observed at 10 Gy (3.27-fold at 24 h and 3.64-fold at 72 h, respectively). Dose-response relationships were significant at both 24 h (Pearson $r=0.52$, $P=1.34x10^{-3}$; Spearman $\rho=0.62$, $P=7.47x10^{-5}$) and 72 h (Pearson $r=0.53$, $P=1.12x10^{-4}$; Spearman $\varrho=0.54$, $P=7.68x10^{-5}$). Urinary MDA likewise increased after irradiation, reaching a 2.87-fold elevation at 7 Gy ($P=5.61x10^{-3}$) (Fig. 2C and D). For urinary MDA, the first significant increase was also observed at 7 Gy at 24 h. Dose–response correlations were significant at 24 h (Pearson $r=0.64$, $P=2.98x10^{-5}$; Spearman $\rho=0.69$, $P=5.39x10^{-5}$). At 72 h, the association remained significant by Pearson correlation ($r=0.38$, $P=7.83x10^{-3}$), whereas Spearman analysis did not reach statistical significance ($\rho=0.23$, $P=0.12$), suggesting increased inter-individual variability at the later time point. A positive association between urinary 8-OHdG and MDA was observed at 24 h (Fig. 3). Receiver operating characteristic (ROC) analysis showed good discrimination of high-dose irradiation (≥7 Gy) from lower doses (≤6 Gy) (Fig. S1): urinary 8-OHdG (AUC=0.84 at 24 h; AUC=0.83 at 72 h) and urinary MDA at 24 h (AUC=0.84) (Fig. S1).

Bone marrow and spleen were primary sources of 8-OHdG and MDA. To identify the tissues contributing to urinary excretion, levels of 8-OHdG and MDA were quantified in

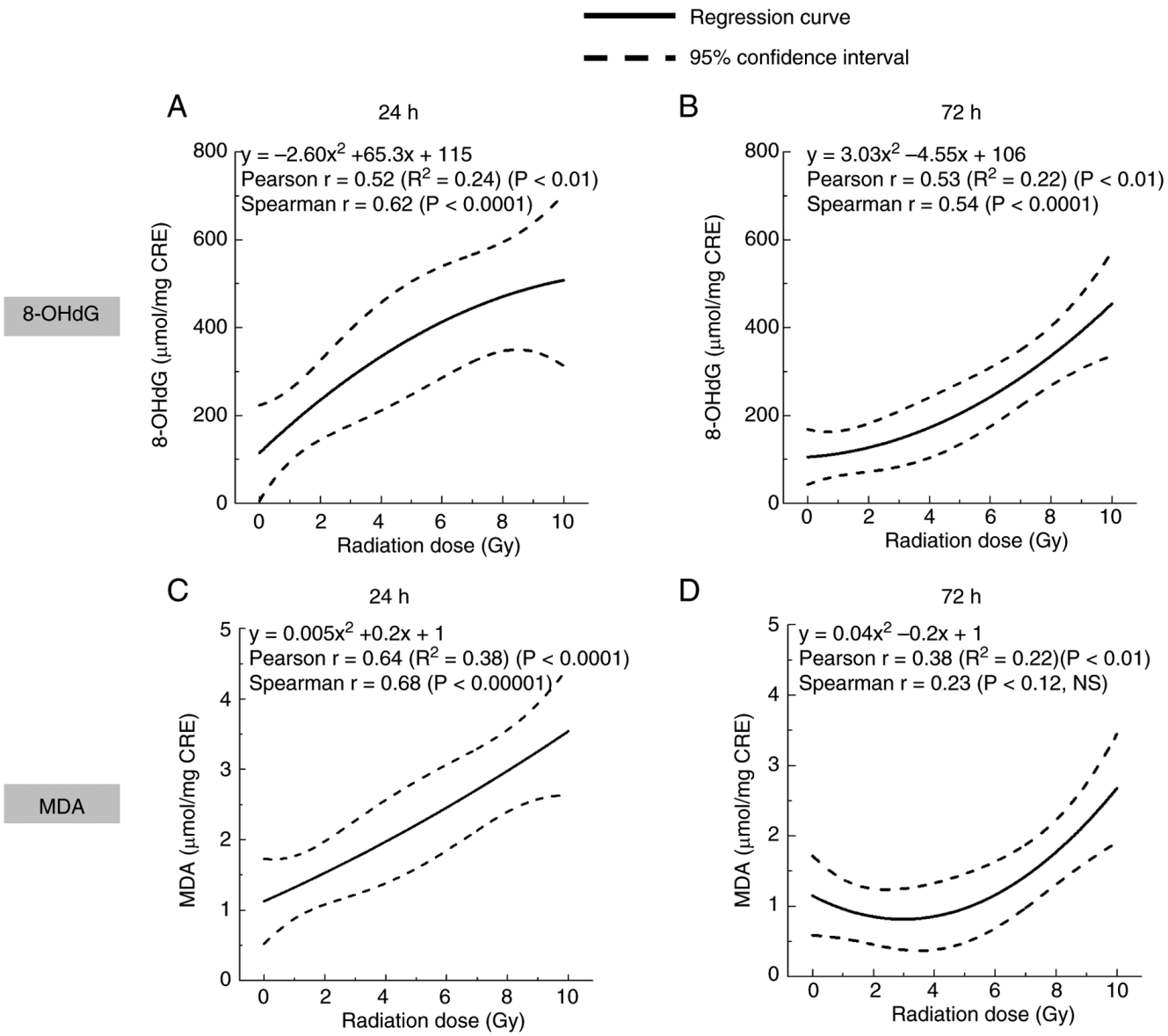

Figure 2. Dose-response profiles of urinary 8-OHdG and MDA. Urine was collected 24 or 72 h after X-irradiation. Urinary 8-OHdG at (A) 24 and (B) 72 h, and urinary MDA at (C) 24 and (D) 72 h. Data were fitted using regression analysis (linear or quadratic as appropriate). Pearson r and Spearman ϱ values (with corresponding P-values) are indicated in each panel. Dashed lines denote 95% confidence intervals. Solid lines represent the selected best-fit model based on R^2 and residual patterns, with preference for the simpler model unless a clear improvement in fit was observed. The reported R^2 values correspond to the selected regression model. 8-OHdG, 8-hydroxy-2'-deoxyguanosine; MDA, malondialdehyde; NS, not significant.

multiple organs after 7 Gy irradiation (Fig. 4). Compared with controls, 8-OHdG increased markedly in spleen and bone marrow ($P=1.33x10^{-3}$ and $P=5.17x10^{-4}$, respectively). MDA levels also increased significantly in bone marrow ($P=5.09x10^{-3}$). Thus, 8-OHdG increased in spleen and bone marrow, and MDA increased in bone marrow after 7 Gy irradiation (Fig. 4A and B).

Dose-dependent release of 8-OHdG and MDA from bone marrow cell cultures. In vitro bone marrow cell cultures revealed a dose-dependent extracellular release of oxidative metabolites (Fig. 5). Bone marrow cultures were irradiated at 0, 2, 4, and 7 Gy (Fig. 5). Supernatant 8-OHdG increased at 4 Gy ($P=4.35x10^{-2}$), and MDA levels increased at 2 to 4 Gy ($P=8.77x10^{-4}$ and $P=1.93x10^{-4}$, respectively). Notably, supernatant MDA at 7 Gy was lower than that at 4 Gy (Fig. 5B).

Radiation-induced apoptosis and necrosis in bone marrow cells. To evaluate radiation-induced DNA damage, a comet assay was performed (Figs. 6 and S2). At a lethal dose of 7 Gy, the tail moment increased significantly, approximately 2.13-fold compared with controls ($P=5.24x10^{-3}$). In addition, flow cytometric analysis revealed in Annexin V+/PI+ late apoptosis at 7 Gy (Fig. 7; $P=1.01x10^{-9}$) in 8-week-old mice. Overall, irradiation was associated with dose-dependent changes in cell death profiles in bone marrow cells (Fig. 7).

Discussion

This study demonstrates that urinary 8-OHdG and TBARS (MDA equivalents) levels increase in a dose- and time-dependent manner, with a sharp rise at ≥7 Gy within the

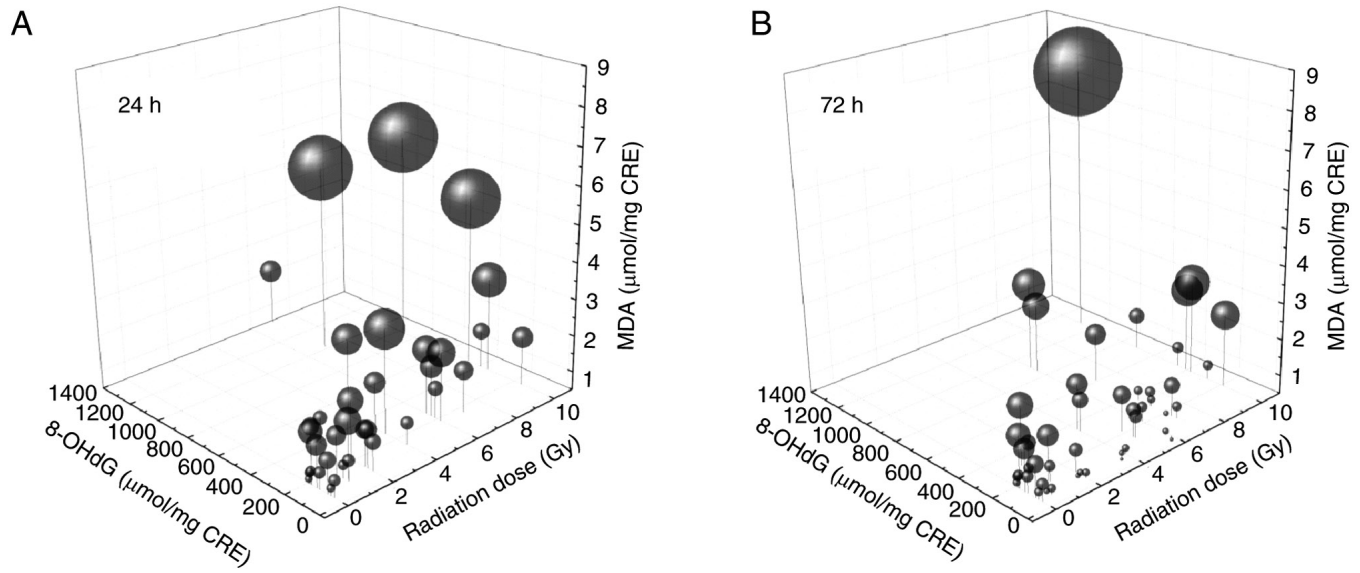

Figure 3. Three-dimensional relationships among radiation dose, urinary 8-OHdG and MDA at (A) 24 and (B) 72 h post-irradiation. Sphere size is proportional to the urinary MDA concentration, with larger spheres indicating higher MDA levels. 8-OHdG, 8-hydroxy-2'-deoxyguanosine; MDA, malondialdehyde.

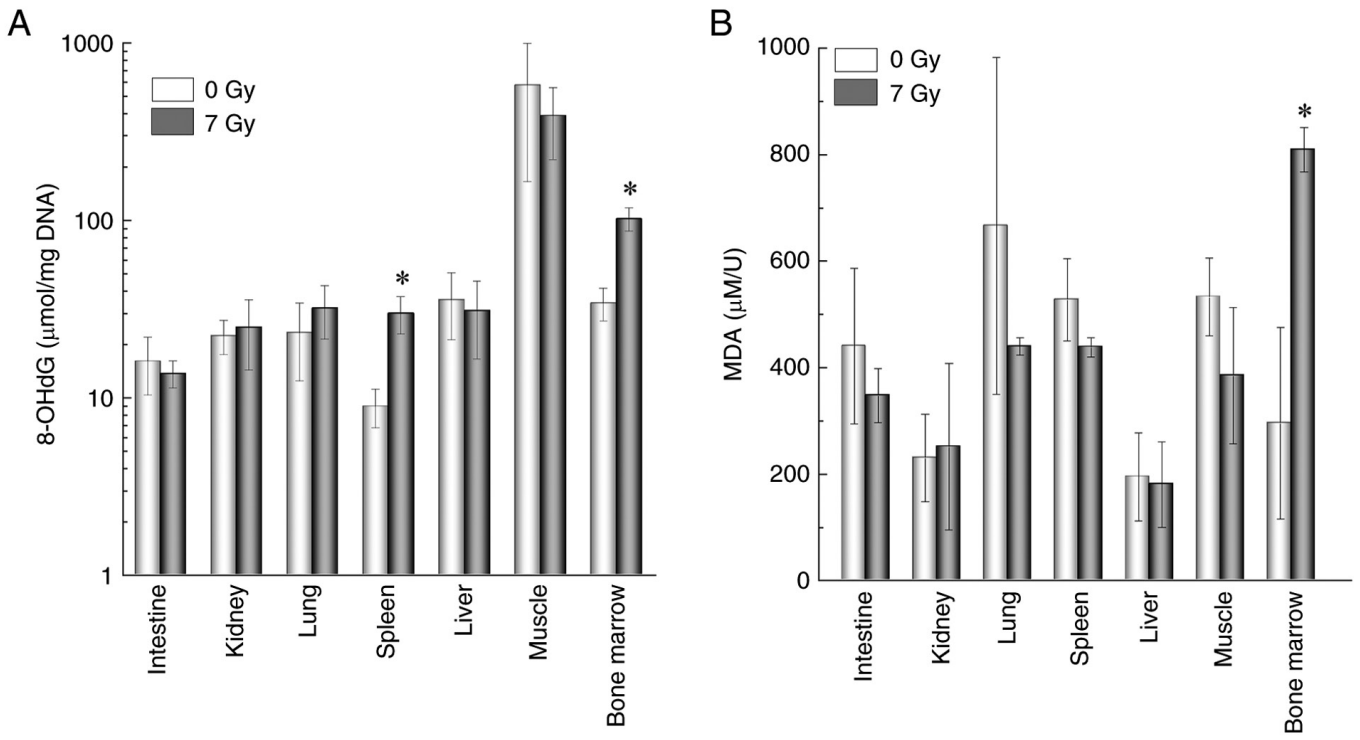

Figure 4. Tissue concentrations of oxidative stress markers at 24 h after 7 Gy irradiation. Quantification of (A) 8-OHdG (μmol/mg DNA) and (B) MDA (μM/U) in multiple organs. Data are presented as the mean ± standard deviation. *P<0.05 vs. 0 Gy. 8-OHdG, 8-hydroxy-2'-deoxyguanosine; MDA, malondialdehyde.

severe exposure range of this murine model. Tissue analyses suggested that the bone marrow and spleen are major contributors to these oxidative damage markers under the conditions tested, and bone marrow cell culture confirmed their extracellular release after irradiation. Flow cytometry further revealed a transition from apoptosis to necrosis at higher doses, offering a mechanistic explanation for the observed metabolite dynamics. Collectively, these findings support urinary 8-OHdG and TBARS as promising biomarkers for biodosimetry in a murine ARS model.

Urinary 8-OHdG has long been established as a sensitive biomarker of oxidative DNA damage in human clinical and epidemiological studies (14-16). Clinical investigations have also reported increased urinary 8-OHdG levels following medical radiation exposures, such as pediatric cardiac catheterization (17) and intensive chemoradiotherapy (15). However, most prior studies have examined diagnostic, therapeutic, or occupational exposure contexts rather than acute high-dose whole-body irradiation. In the present murine ARS model, we observed marked threshold-like increases in

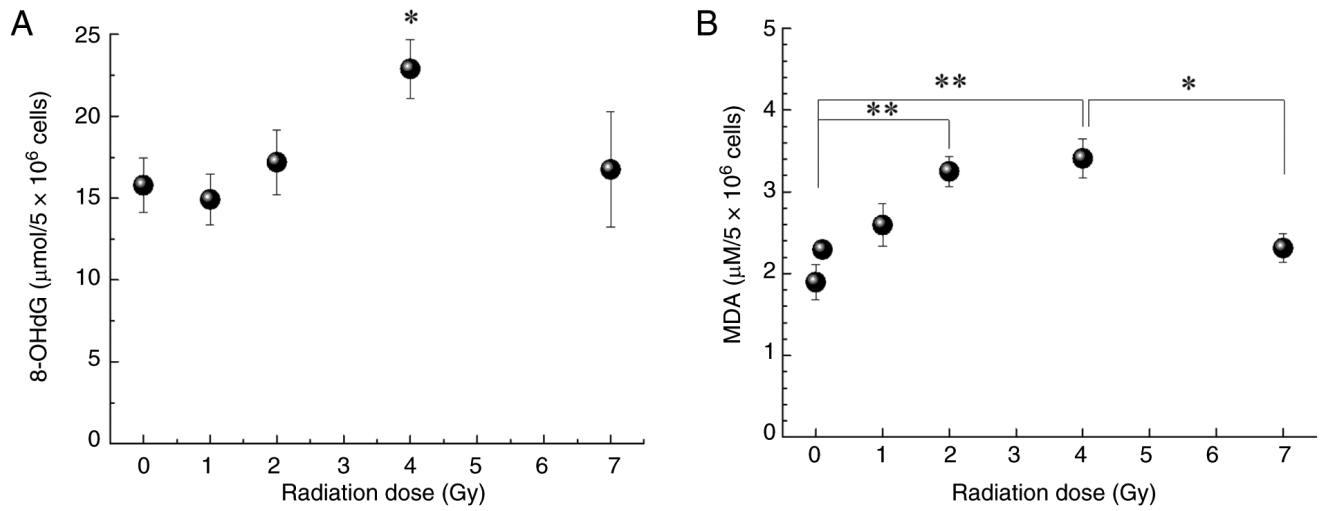

Figure 5. Release of oxidative metabolites from bone marrow cell cultures. Freshly isolated bone marrow cells from irradiated mice were cultured for 24 h, and the concentrations of (A) 8-OHdG and (B) MDA in the culture supernatant were quantified. Values are expressed per 5x10^6 cells (normalized to a fixed number of cells). Data are presented as the mean ± standard deviation. *P<0.05, **P<0.01 vs. 0 Gy (Tukey-Kramer multiple comparison test). 8-OHdG, 8-hydroxy-2'-deoxyguanosine; MDA, malondialdehyde.

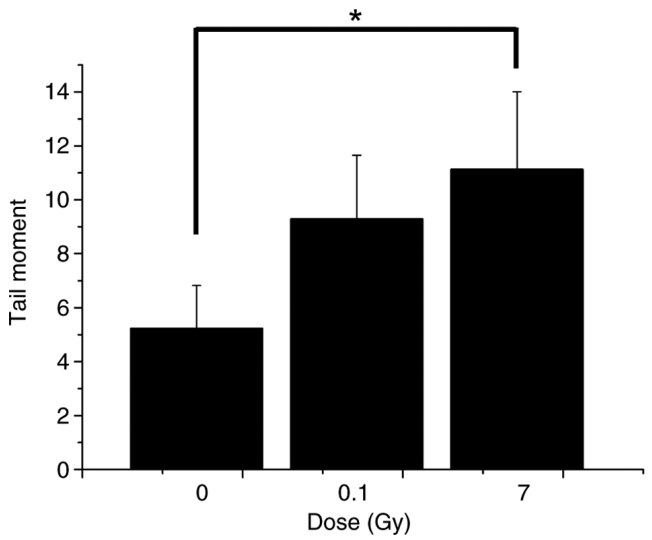

Figure 6. DNA damage in irradiated bone marrow cells assessed using the comet assay. Tail moment was measured in cultured bone marrow cells 24 h after irradiation. Data are presented as the mean ± standard deviation. *P<0.05 vs. 0 Gy (Tukey-Kramer multiple comparison test).

urinary 8-OHdG within the 7-10 Gy range tested, together with clear dose-response relationships. By contrast, evidence for urinary TBARS following IR is comparatively limited, with many reports focusing on UV exposure or chemically induced oxidative stress models (20). Here, urinary TBARS increased in a dose-dependent manner after X-irradiation, paralleling the elevation of 8-OHdG. The concurrent increase in markers of oxidative DNA damage and lipid peroxidation at higher doses supports their potential complementary utility in radiation-induced oxidative injury assessment.

The observed metabolite elevations align with the central role of ROS in radiation injury. Hydroxyl radicals generated by water radiolysis oxidize guanine to 8-OHdG (10,11), whereas lipid peroxidation generates aldehydic products including MDA which are commonly assessed as TBARS (12,13). The marked increases in bone marrow and spleen are consistent with the well-recognized radiosensitivity of these tissues (1). *In vitro* bone marrow cultures confirmed the dose-dependent extracellular release of both metabolites, and the decline in TBARS at 7 Gy occurred in parallel with an increased necrotic fraction. Although only limited dose points were examined, this observation may be consistent with a shift in the predominant mode of cell death under severe injury conditions; however, this interpretation should be considered exploratory and requires validation across additional dose levels. Interestingly, *in vitro* TBARS levels declined at 7 Gy despite continued increases observed *in vivo*. This apparent discrepancy may reflect differences between systemic and cell culture conditions. *In vivo*, urinary TBARS represents the integrated contribution of multiple irradiated tissues and ongoing oxidative metabolism. In contrast, *in vitro* measurements reflect extracellular release from isolated bone marrow cells. At very high doses, the shift from apoptosis to necrosis may alter membrane integrity and overall cellular metabolism, which could influence extracellular metabolite profiles. Additionally, TBARS readouts in cell culture supernatants may be influenced by other thiobarbituric acid–reactive species under extreme oxidative conditions.

Temporal dynamics should also be considered when interpreting these biomarkers. At 24 h after irradiation, both urinary 8-OHdG and TBARS showed strong dose-response correlations, consistent with acute ROS generation and oxidative macromolecular damage. By 72 h, although elevated levels persisted, the strength of correlation decreased, particularly for TBARS, where rank-based correlation did not remain significant at 72 h. This attenuation may reflect the transition from acute oxidative burst to secondary biological responses, including DNA repair, antioxidant activation, cellular clearance, and inter-individual variability in tissue recovery. As systemic metabolism and excretion mechanisms contribute increasingly over time, biomarker levels may become influenced by additional physiological factors beyond initial radiation dose. These findings suggest that the 24 h time point may provide a more robust window for dose discrimination,

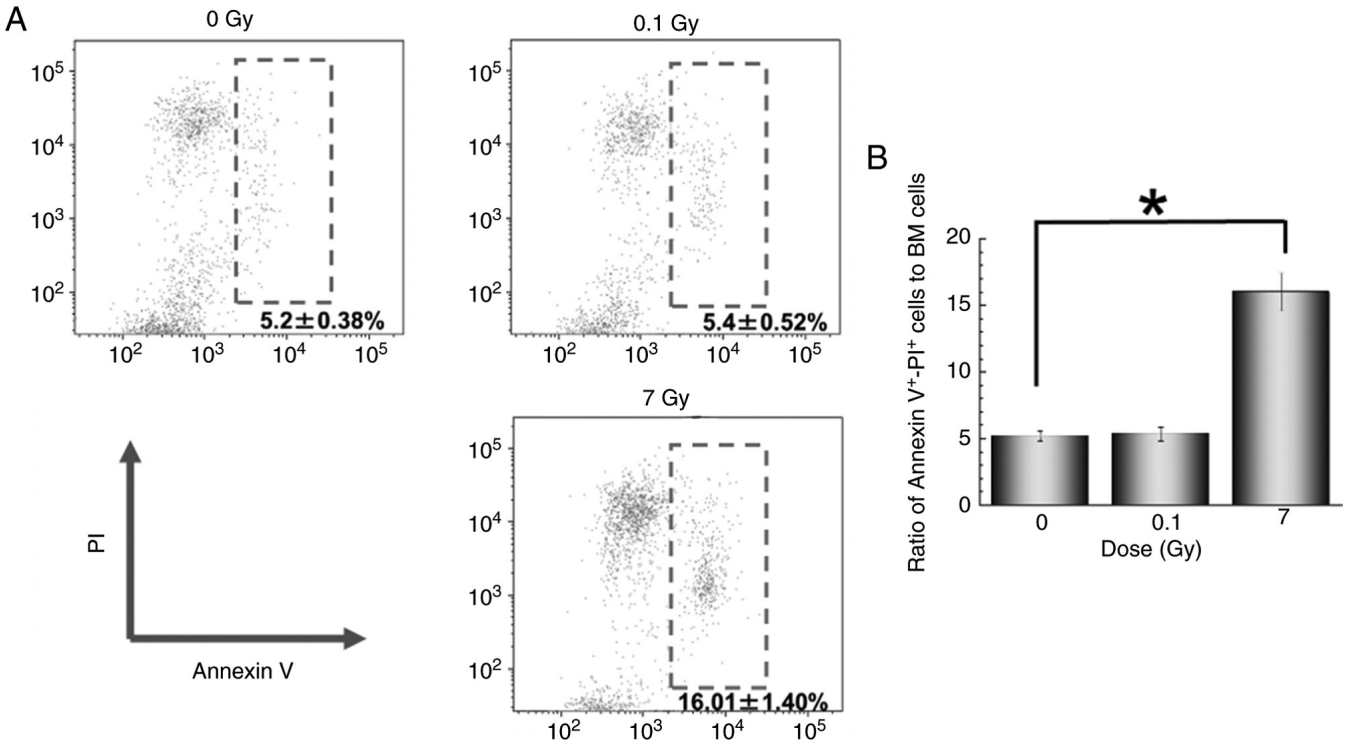

Figure 7. Apoptosis and necrosis in BM cells after X-irradiation. BM cells were collected 24 h after irradiation of 8-week-old mice, stained with annexin V-FITC and PI, and analyzed by flow cytometry. (A) Representative quadrant dot plots. (B) Quantification of annexin V^+/PI^+ (late apoptotic) populations. Data are presented as the mean ± standard deviation. *P<0.05 vs. 0 Gy (Tukey-Kramer multiple comparison test). BM, bone marrow.

whereas later measurements reflect a more complex interplay between damage and recovery processes.

Radiation metabolomics has emerged as a powerful approach for biodosimetry. Several studies in murine and nonhuman primate irradiation models have documented dose-dependent changes in urinary metabolites (8,9,26,27). For instance, Pannkuk *et al* (9) (mouse total-body irradiation model) and Golla *et al* (8) (nonhuman primate irradiation model) reported perturbations in tricarboxylic acid (TCA) cycle intermediates and amino acids after total-body irradiation. Importantly, metabolomic profiling of urine from patients undergoing total-body irradiation revealed radiation-responsive signatures overlapping with animal findings, underscoring the translational potential of this approach (28). Recent reviews highlight that combining targeted oxidative markers such as 8-OHdG and TBARS with untargeted metabolomics may enhance the robustness and specificity of radiation biodosimetry (26,29). In addition to metabolomic signatures, practical triage requires interpretable links between biological injury severity and clinical decision domains. To provide clinical context without implying direct interspecies dose equivalence, we present a conceptual mapping between the murine dose range investigated and the corresponding hematopoietic injury domains in human ARS (Table SI). This contextualization is intended to illustrate the relative biological severity domain rather than to suggest quantitative dose conversion. In this framework, the ≥7 Gy range in our murine model corresponds to a severe hematopoietic injury domain characterized by pronounced oxidative stress and cell death dynamics, which is relevant for early high-risk stratification in radiation emergency settings. Given known species differences in radiosensitivity, this mapping should be interpreted cautiously and serves primarily as a translational orientation tool.

Rapid discrimination between individuals at risk of severe hematopoietic injury is critical in radiological or nuclear incidents, including high-dose criticality events such as the JCO accident in Japan. In such settings, early triage relies on clinical presentation and readily available laboratory parameters, while definitive dose reconstruction typically requires cytogenetic biodosimetry (3,6). Although chromosomal aberration analysis remains highly accurate, it requires several days to complete. In contrast, urinary 8-OHdG and TBARS can be quantified within hours using relatively simple immunochromatographic or colorimetric assays. Therefore, these markers may serve as adjunct tools for early risk stratification, providing rapid, noninvasive indications of systemic oxidative injury while confirmatory biodosimetry is pending. Their dose-dependent elevations and association with bone marrow injury suggest potential utility in guiding early supportive interventions. Preliminary ROC analysis further supported the discriminatory capacity of urinary 8-OHdG for identifying high-dose exposure (Fig. S1), although validation in larger datasets will be required to establish clinically actionable cutoff values. Given the controlled preclinical setting and limited sample size, provisional cut-off values and multivariable models were not derived to avoid unstable estimates. Larger independent cohorts will be required to define clinically actionable thresholds and assess combined-marker performance.

These findings were obtained under tightly controlled experimental conditions (diet, housing, and sampling schedule), and therefore the impact of inter-individual confounders such as diet, renal function, microbiome composition, and mixed injuries should be evaluated in future translational studies. In

addition, this study was conducted in mice, and validation in humans-particularly in patients undergoing high-dose radiotherapy or total-body irradiation-is essential before clinical implementation. Species differences in radiosensitivity, baseline urinary excretion, renal handling of oxidative metabolites, and systemic inflammatory responses may influence both absolute biomarker levels and optimal sampling windows. Human validation should proceed stepwise: i) evaluation in controlled clinical exposure settings; ii) analytical verification using orthogonal methods (e.g., LC-MS-based quantification) with inter-laboratory reproducibility; and iii) prospective assessment of diagnostic performance and clinically actionable thresholds for emergency triage. Differences between low-LET and high-LET radiation may further influence oxidative biomarker kinetics and should also be investigated.

Second, the TBARS assay for MDA is not fully specific, because thiobarbituric acid can react with other aldehydes and lipid peroxidation-derived products in addition to MDA. Therefore, the measured values should be interpreted as TBARS rather than absolute MDA concentrations, and non-specific reactions may lead to overestimation, particularly under high-dose irradiation where oxidative reactions are amplified. Importantly, TBARS non-specificity is expected to influence absolute values more than relative dose-response patterns when samples are processed under identical conditions with consistent timing and internal controls. In this study, TBARS is therefore interpreted primarily as an index of lipid peroxidation dynamics across dose groups rather than a definitive quantification of MDA. Nevertheless, the consistent dose-dependent increase at 24 h and the significant association with radiation dose support its utility as a practical oxidative stress indicator in this experimental biodosimetry setting. LC-MS/HPLC-based quantification was not performed in the present study, and future work should validate these findings using more specific analytical methods. Formal cutoff determination and external validation will also be required to establish clinically actionable diagnostic thresholds. In addition, confounding factors such as diet, renal function, and microbiome composition may influence urinary metabolite levels (18,30). Recent work shows that microbiome depletion alters biofluid metabolite responses to irradiation (30), highlighting interindividual variability as a key challenge for clinical translation.

In conclusion, in this murine model of severe whole-body irradiation, urinary 8-OHdG and TBARS showed clear dose- and time-dependent increases with a sharp rise at ≥7 Gy. These findings support their potential utility as rapid, noninvasive adjunct biomarkers for early risk stratification in radiation emergencies, pending validation in larger and human cohorts.

Acknowledgements

Not applicable.

Funding

The present study was supported by JSPS KAKENHI, Grants-in-Aid for Scientific Research (B) (grant no. 21H02861/23K21419), Grant-in-Aid for Challenging Research (grant no. 25K22722) and Takeda Science Foundation 2023.

Availability of data and materials

The data generated in the present study are included in the figures and/or tables of this article.

Authors' contributions

SM, KT and YT designed the study, prepared the manuscript draft and substantively participated in the manuscript revision. SM, KT, YT, TS and NK analyzed all biological data. SM and YM supervised the study, contributed to data interpretation, critically revised the manuscript for important intellectual content, and provided final approval for the version to be submitted and published. SM and YM confirm the authenticity of all the raw data and take responsibility for the integrity of the data. All authors have read and approved the final version of the manuscript.

Ethics approval and consent to participate

All animal experiments were conducted in accordance with institutional guidelines for animal care and use and approved by the Animal Research Committee of Hirosaki University (approval no. G12003; Hirosaki, Japan).

Patient consent for publication

Not applicable.

Competing interests

The authors declare that they have no competing interests.

References

1. Chiba S, Saito A, Ogawa S, Takeuchi K, Kumano K, Seo S, Suzuki T, Tanaka Y, Saito T, Izutsu K, *et al*: Transplantation for accidental acute high-dose total body neutron- and gamma-radiation exposure. Bone Marrow Transplant 29: 935-939, 2002.
2. Radiation Emergency Medical Preparedness and Assistance Network (REMPAN). https://www.who.int/groups/rempan. Accessed February 25, 2026.
3. IAEA. Cytogenetic dosimetry: Applications in preparedness for and response to radiation emergencies (EPR-Biodosimetry 2011). Vienna: IAEA, 2011.
4. North Atlantic Treaty Organization: AMedP-7: Medical Management of CBRN Casualties. Edition A, Version 1. Brussels: NATO Standardization Office, Brussels, Belgium, 2018.
5. Kulka U, Ainsbury L, Atkinson M, Barnard S, Smith R, Barquinero JF, Barrios L, Bassinet C, Beinke C, Cucu A, *et al*: Realising the European network of biodosimetry: RENEB-status quo. Radiat Prot Dosimetry 164: 42-45, 2015.
6. No authors listed: The 2007 recommendations of the international commission on radiological protection. ICRP publication 103. Ann ICRP 37: 1-332, 2007.
7. Schley G, Köberle C, Manuilova E, Rutz S, Forster C, Weyand M, Formentini I, Kientsch-Engel R, Eckardt KU and Willam C: Comparison of plasma and urine biomarker performance in acute kidney injury. PLoS One 10: e0145042, 2015.
8. Golla S, Golla JP, Krausz KW, Manna SK, Simillion C, Beyoğlu D, Idle JR and Gonzalez FJ: Metabolomic analysis of mice exposed to gamma radiation reveals a systemic understanding of total-body exposure. Radiat Res 187: 612-629, 2017.
9. Pannkuk EL, Laiakis EC, Authier S, Wong K and Fornace AJ Jr: Gas chromatography/mass spectrometry metabolomics of urine and serum from nonhuman primates exposed to ionizing radiation: Impacts on the tricarboxylic acid cycle and protein metabolism. J Proteome Res 16: 2091-2100, 2017.

10. Crouch JD and Brosh RM Jr: Mechanistic and biological considerations of oxidatively damaged DNA for helicase-dependent pathways of nucleic acid metabolism. Free Radic Biol Med 107: 245-257, 2017.
11. Haghdoost S, Czene S, Näslund I, Skog S and Harms-Ringdahl M: Extracellular 8-oxo-dG as a sensitive parameter for oxidative stress in vivo and in vitro. Free Radic Res 39: 153-162, 2005.
12. Ayala A, Muñoz MF and Argüelles S: Lipid peroxidation: Production, metabolism, and signaling mechanisms of malondialdehyde and 4-hydroxy-2-nonenal. Oxid Med Cell Longev 2014: 360438, 2014.
13. Tsikas D: Assessment of lipid peroxidation by measuring malondialdehyde (MDA) and relatives in biological samples: Analytical and biological challenges. Anal Biochem 524: 13-30, 2017.
14. Loft S and Poulsen HE: Cancer risk and oxidative DNA damage in man. J Mol Med (Berl) 74: 297-312, 1996.
15. Bergman V, Leanderson P, Starkhammar H and Tagesson C: Urinary excretion of 8-hydroxydeoxyguanosine and malondialdehyde after high dose radiochemotherapy preceding stem cell transplantation. Free Radic Biol Med 36: 300-306, 2004.
16. Graille M, Wild P, Sauvain JJ, Hemmendinger M, Guseva Canu I and Hopf NB: Urinary 8-OHdG as a biomarker for oxidative stress: A systematic literature review and meta-analysis. Int J Mol Sci 21: 3743, 2020.
17. Kato S, Yoshimura K, Kimata T, Mine K, Uchiyama T and Kaneko K: Urinary 8-hydroxy-2'-deoxyguanosine: A biomarker for radiation-induced oxidative DNA damage in pediatric cardiac catheterization. J Pediatr 167: 1369-1374.e1, 2015.
18. Chiba M, Monzen S, Iwaya C, Kashiwagi Y, Yamada S, Hosokawa Y, Mariya Y, Nakamura T and Wojcik A: Serum miR-375-3p increase in mice exposed to a high dose of ionizing radiation. Sci Rep 8: 1302, 2018.
19. Monzen S, Terada K, Morino Y and Chiba M: Urinal biomarker, 8-Hydroxy-2'-Deoxyguanosine,for unexpected exposure dose of ionizing radiation. Cytometry Res 28: 41-45, 2018 (In Japanese)..
20. Williams JD, Bermudez Y, Park SL, Stratton SP, Uchida K, Hurst CA and Wondrak GT: Malondialdehyde-derived epitopes in human skin result from acute exposure to solar UV and occur in nonmelanoma skin cancer tissue. J Photochem Photobiol B 132: 56-65, 2014.
21. Waselenko JK, MacVittie TJ, Blakely WF, Pesik N, Wiley AL, Dickerson WE, Tsu H, Confer DL, Coleman CN, Seed T, *et al*: Medical management of the acute radiation syndrome: Recommendations of the strategic national stockpile radiation working group. Ann Intern Med 140: 1037-1051, 2004.
22. Centers for Disease Control and Prevention: Acute Radiation Syndrome: Information for Clinicians. https://www.cdc.gov/radiation-emergencies/hcp/clinical-guidance/ars.html Accessed February 24, 2026.
23. Singh VK, Romaine PLP and Newman VL: Biologics as countermeasures for acute radiation syndrome: Where are we now? Expert Opin Biol Ther 15: 465-471, 2015.
24. Satyamitra M, Kumar VP, Biswas S, Cary L, Dickson L, Venkataraman S and Ghosh SP: Impact of abbreviated filgrastim schedule on survival and hematopoietic recovery after irradiation in four mouse strains with different radiosensitivity. Radiat Res 187: 659-671, 2017.
25. Nunamaker EA, Artwohl JE, Anderson RJ and Fortman JD: Endpoint refinement for total body irradiation of C57BL/6 mice. Comp Med 63: 22-28, 2013.
26. Johnson CH, Patterson AD, Krausz KW, Kalinich JF, Tyburski JB, Kang DW, Luecke H, Gonzalez FJ, Blakely WF and Idle JR: Radiation metabolomics. 5. Identification of urinary biomarkers of ionizing radiation exposure in nonhuman primates by mass spectrometry-based metabolomics. Radiat Res 178: 328-340, 2012.
27. Coy SL, Cheema AK, Tyburski JB, Laiakis EC, Collins SP and Fornace AJ Jr: Radiation metabolomics and its potential in biodosimetry. Int J Radiat Biol 87: 802-23, 2011.
28. Laiakis EC, Mak TD, Anizan S, Amundson SA, Barker CA, Wolden SL, Brenner DJ and Fornace AJ Jr: Development of a metabolomic radiation signature in urine from patients undergoing total body irradiation. Radiat Res 181: 350-361, 2014.
29. Satyamitra MM, Cassatt DR, Hollingsworth BA, Price PW, Rios CI, Taliaferro LP, Winters TA and DiCarlo AL: Metabolomics in radiation biodosimetry: Current approaches and advances. Metabolites 10: 328, 2020.
30. Pannkuk EL, Shuryak I, Kot A, Lin LYT, Li HH and Fornace AJ Jr: Host microbiome depletion attenuates biofluid metabolite responses following radiation exposure. PLoS One 19: e0300883, 2024.